Supplementary Information (SI) for Journal of Materials Chemistry C.

Supporting Information

Rapid-photo-responsive photoluminescence of spiropyran-encapsulated cage-like zeolitic imidazolate frameworks via dynamic energy transfer process

Zheyan Xu [a], He-Qi Zheng [b,*], Shijun Wang [a], Chenyu Li [a], Guodong Qian [a] and Yuanjing Cui [a, b, *]

[a]State Key Laboratory of Silicon and Advanced Semiconductor Materials, School of Materials Science & Engineering, Zhejiang University, Hangzhou 310030, China

[b]Zhejiang Provincial Key Laboratory of Optoelectronic Functional Materials and Devices, ZJU-Hangzhou Global Scientific and Technological Innovation Center, School of Materials Science & Engineering, Zhejiang University, Hangzhou 311200, China

E-mail: heqizheng@zju.edu.cn (H.-Q. Zheng); cuiyj@zju.edu.cn (Y. Cui)

1. Experimental Section/Methods

1.1 Chemicals

All the reagents and chemicals were provided by commercial channels. Polydimethylsiloxane (PDMS) was purchased from TCI and used directly without further purification. Purification ultrapure water was prepared with an Aquapro system (18.25 MΩ cm^{-1}).

1.2 Measurement and analysis

Powder X-ray diffraction (PXRD) data were collected on a PANalytical X'Pert Pro X-ray diffractometer using a Cu Kα (λ= 1.542 Å) beam at room temperature with 2θ ranging from 2° to 50°. ^{1}H NMR spectra were recorded on a Bruker AVANCE III500 spectrometer. Thermogravimetric analyses (TGA) were obtained on a Netzsch TG209F3 under N_2 atmosphere with a heating rate of 10 K min^{-1}, the testing temperature was set from 20 ℃ to 800 ℃. The scanning electron microscopy (SEM) images were recorded using a field-emission scanning electron microscopy (FE-SEM, JSM-IT800). Fourier transform infrared (FT-IR) spectra were collected on a Bruker Vertex 70 spectrometer. UV-Vis adsorption spectra of AF and SP were performed on UV-2600 spectrometer (Shimadzu Corp, Japan), the testing range was set from 200 nm to 800 nm. Confocal laser scanning images were taken on an Olympus FV1000 laser scanning confocal microscope equipped with an Olympus IX81 inverted microscope. Fluorescence lifetime measurement was conducted using a 450 nm nanosecond pulsed laser on the Edinburgh FLS1000 spectrophotometer. The photoluminescence quantum yield (PLQY) of all materials was recorded on an Edinburgh FLS1000 spectrophotometer equipped with an integrating sphere and a 450 W xenon lamp as an excitation source. Fluorescence signals of probes were recorded on a Hitachi F4600 fluorescence spectrometer. Xenon lamp serves as an excitation light source. In real experiment, scanning speed was set at 1200 nm·min^{-1}, excitation and emission slits width and detector voltage were adjusted to get a proper fluorescence intensity, the test condition remained constant in the whole experiment. In our experiments, the UV (365 nm) irradiation was provided by a commercial UV lamp. The

light intensity at the sample surface was measured to be 0.61 mW/cm^2, and the illumination distance was fixed at 30 cm.

1.3 Determination of spiropyran and acriflavine contents

The UV-visible spectras of the spiropyran solution and acriflavine solution were measured, and the concentration was calculated through **Equation S1** and **Equation S2**.

$$y_1 = 0.0303x_1 + 0.0711 \quad (1)$$

y_1 - absorption; x_1 - concentration of SP

$$y_2 = 0.164x_2 + 0.0673 \quad (2)$$

y_2 - absorption; x_2 - concentration of AF

The absorptions of different concentration of spiropyran and acriflavine in ethanol solution were measured and repeated three times, and then the average values were calculated. By collecting the solution after centrifugation of the material, testing their absorbances, and calculating their contents through **Equation S1** and **Equation S2**.

Table S1. Quantum yield of AF, ZIF-11⊃AF, spiropyran and ZIF-11⊃MC.

Sample	**Emission (nm)**	**QY (%)**
AF powder	625	≈ 0.00
AF in CH_3OH (3×10^{-5} mol L^{-1})	505	2.45
ZIF-11⊃AF	490	7.10
rho-ZMOF⊃AF	530	16.58
spiropyran powder	525	≈ 0.00
MC in CH_3OH (10^{-4} mol L^{-1})	637	0.10
ZIF-11⊃MC	685	3.36
rho-ZMOF⊃MC	630	1.89

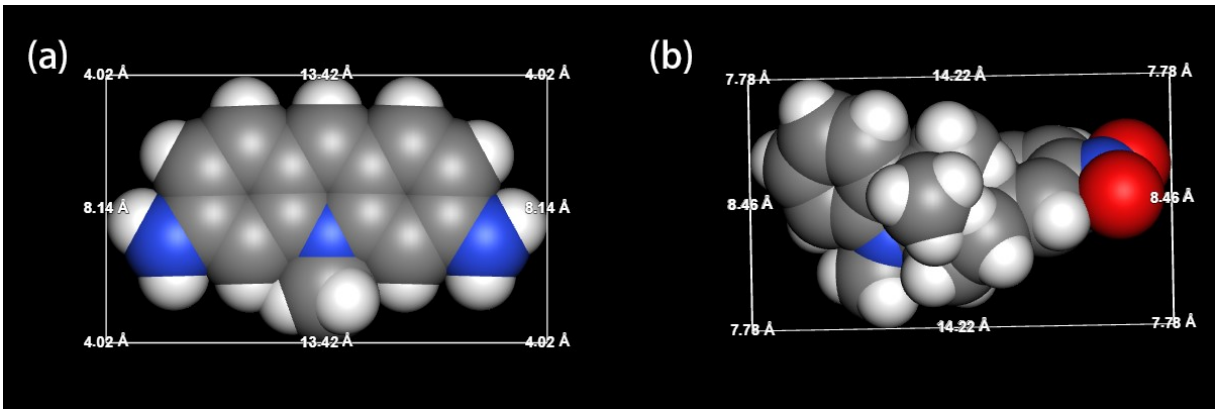

Figure S1. Molecular structures of (a) acriflavine and (b) spiropyran.

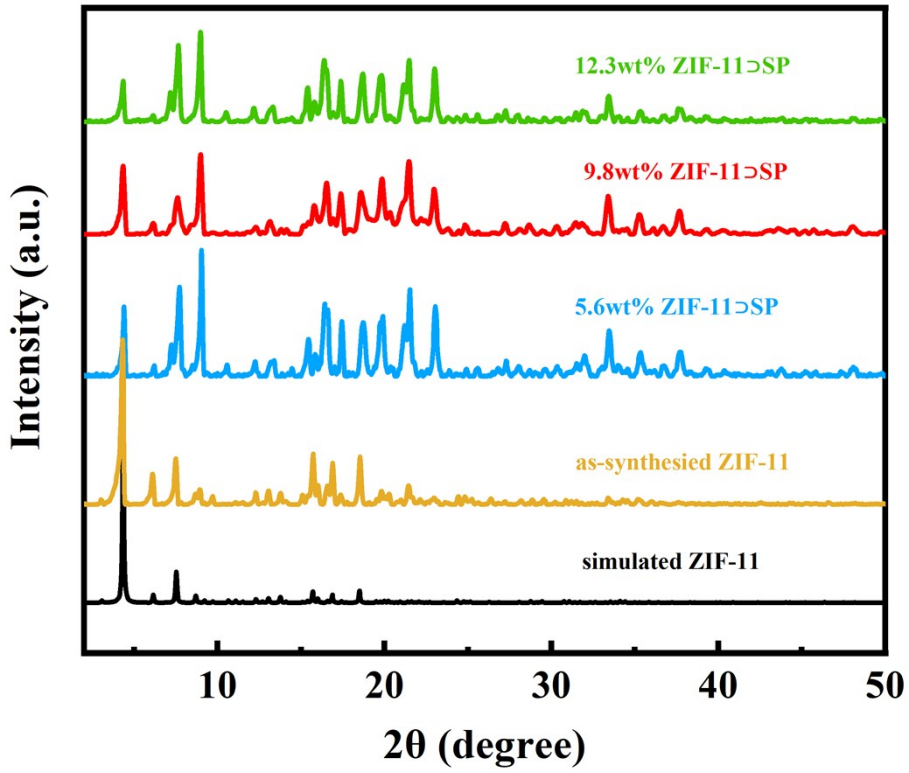

Figure S2. PXRD patterns ZIF-11 and ZIF-11⊃SP with different spiropyran content.

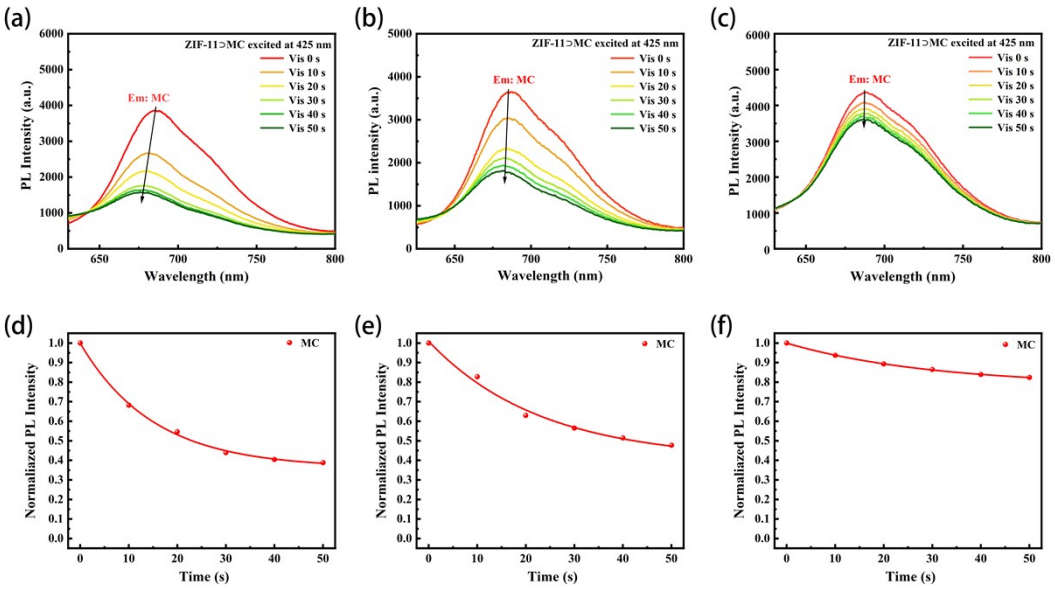

Figure S3. The emission spectra of ZIF-11⊃SP (a) 5.6 wt%, (b) 9.8 wt%, (c) 12.3 wt% with different spiropyran content under visible light irradiation excited at 425 nm. Time-dependent fluorescence intensity of MC in ZIF-11⊃SP (d) 5.6 wt%, (e) 9.8 wt%, (f) 12.3 wt% with different spiropyran content under visible light irradiation.

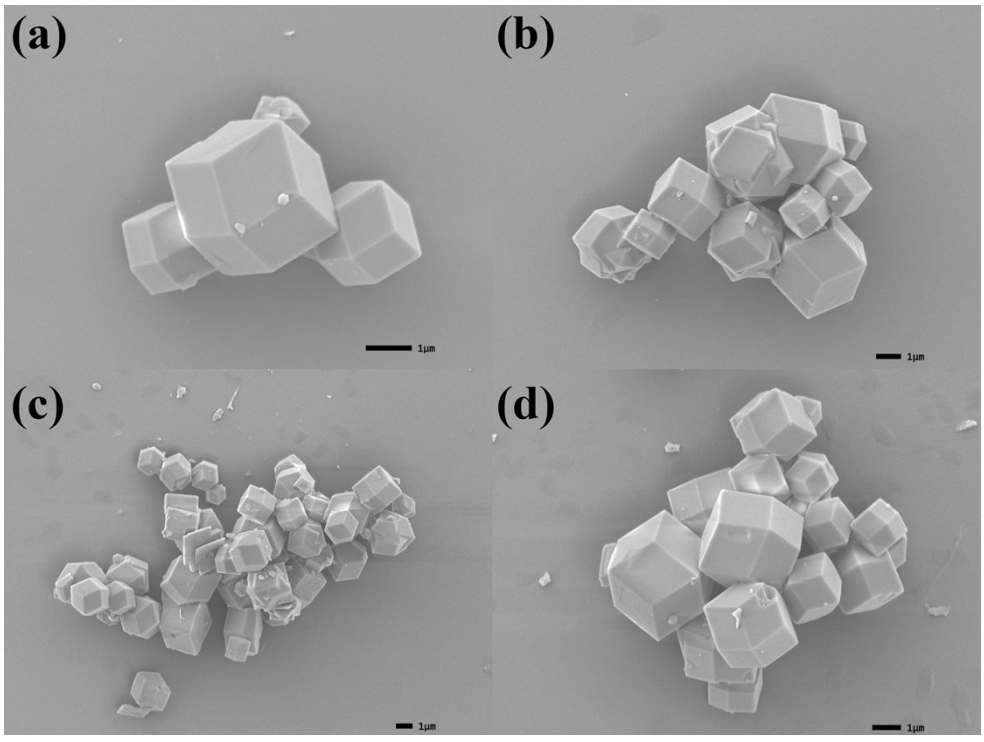

Figure S4. SEM images of (a) ZIF-11, (b) ZIF-11⊃ SP, (c) ZIF-11⊃AF, (d) ZIF-11⊃AF&SP, Scale bar = 1 μm.

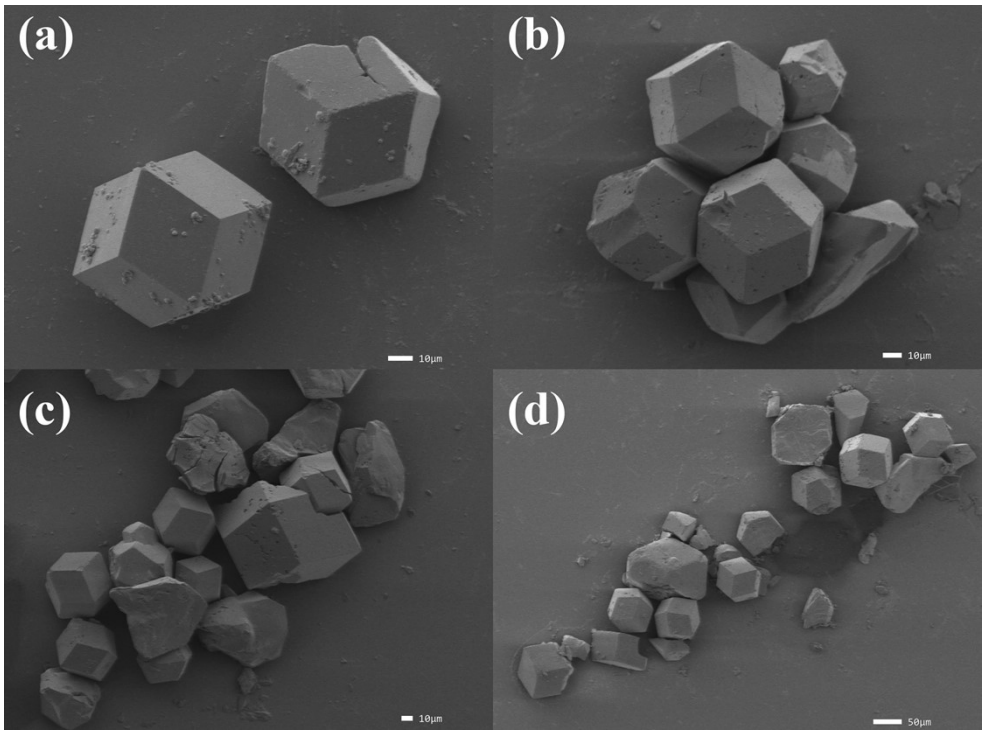

Figure S5. SEM images of (a) rho-ZMOF, (b) rho-ZMOF⊃AF, (c) rho-ZMOF⊃SP, Scale bar = 10 μm, (d) rho-ZMOF⊃AF&SP, Scale bar = 50 μm.

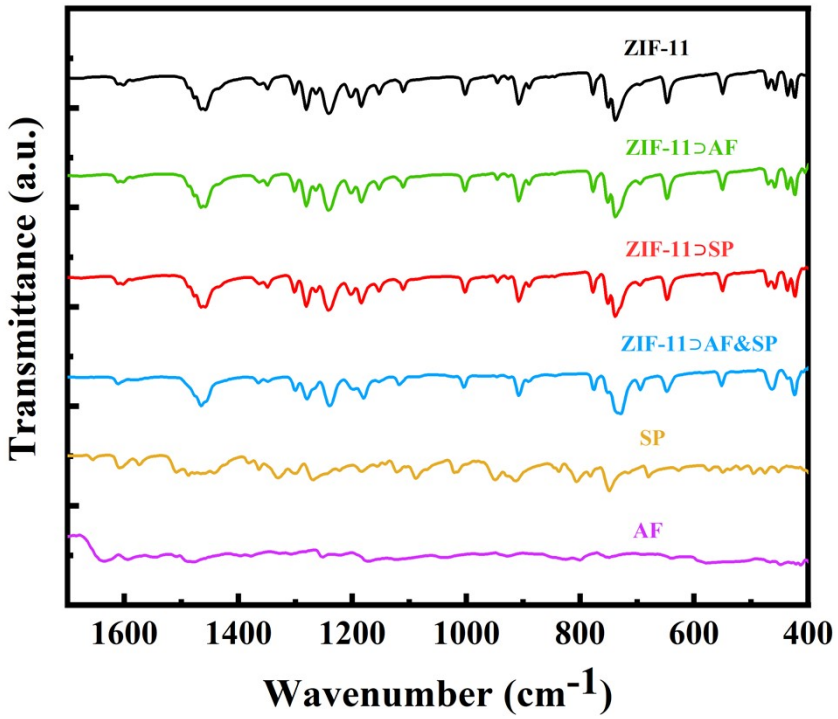

Figure S6. FT-IR spectra of ZIF-11, ZIF-11⊃AF, ZIF-11⊃SP, ZIF-11⊃AF&SP, spiropyran and acriflavine.

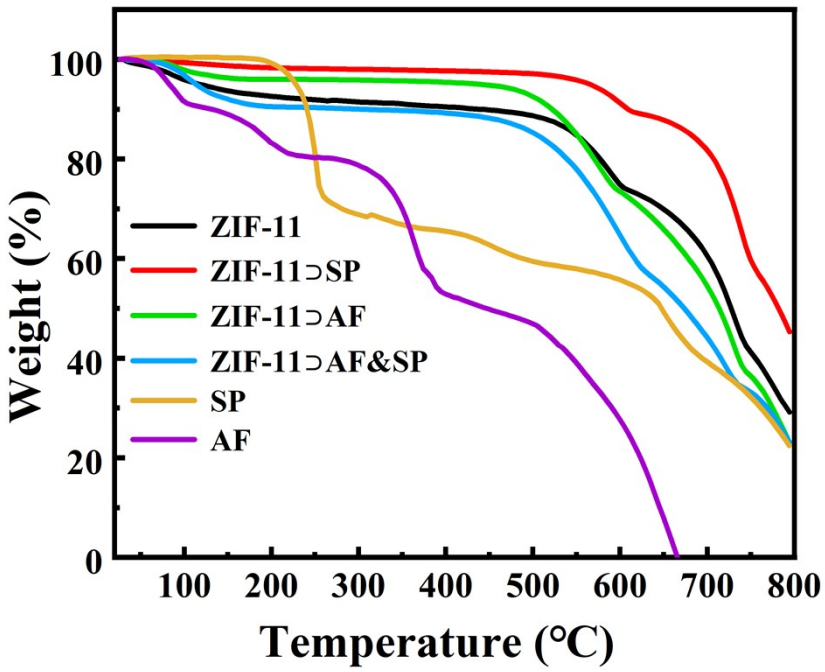

Figure S7. The TGA curve of ZIF-11, ZIF-11⊃AF, ZIF-11⊃SP, ZIF-11⊃AF&SP, spiropyran and acriflavine.

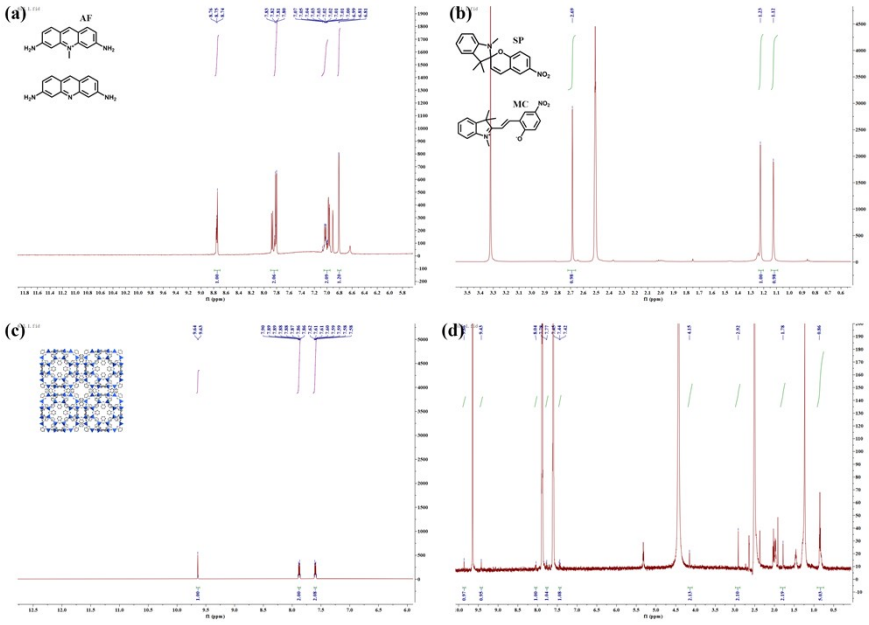

Figure S8. The ^{1}HNMR spectrum of (a) AF, (b) SP, (c) ZIF-11 and (d) ZIF-11⊃AF&SP (solvent DMSO-d_6).

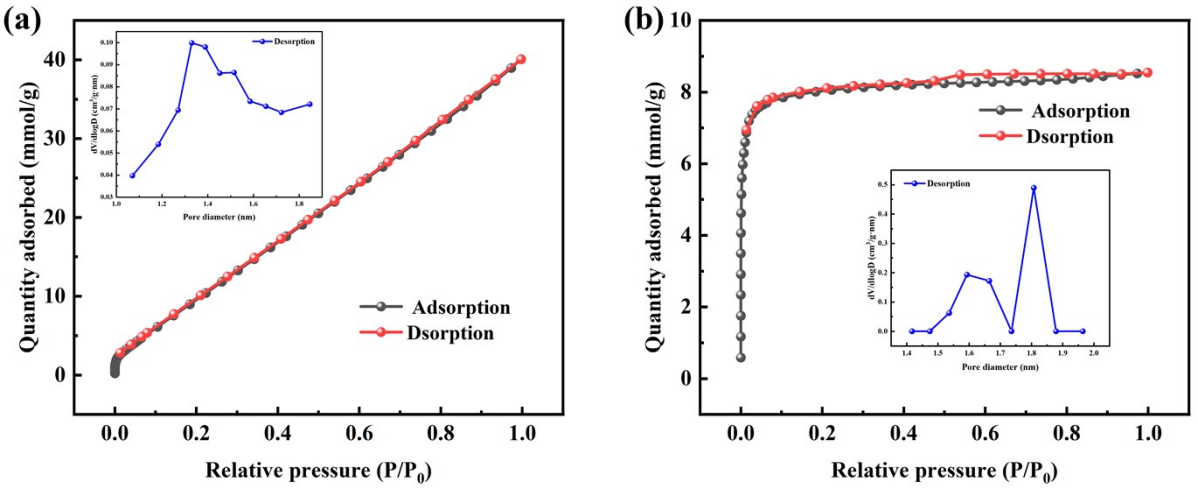

Figure S9. (a) N_2 sorption isotherms of ZIF-11 at 77 K and pore size distribution map. (b) N_2 sorption isotherms of rho-ZMOF at 77 K and pore size distribution map.

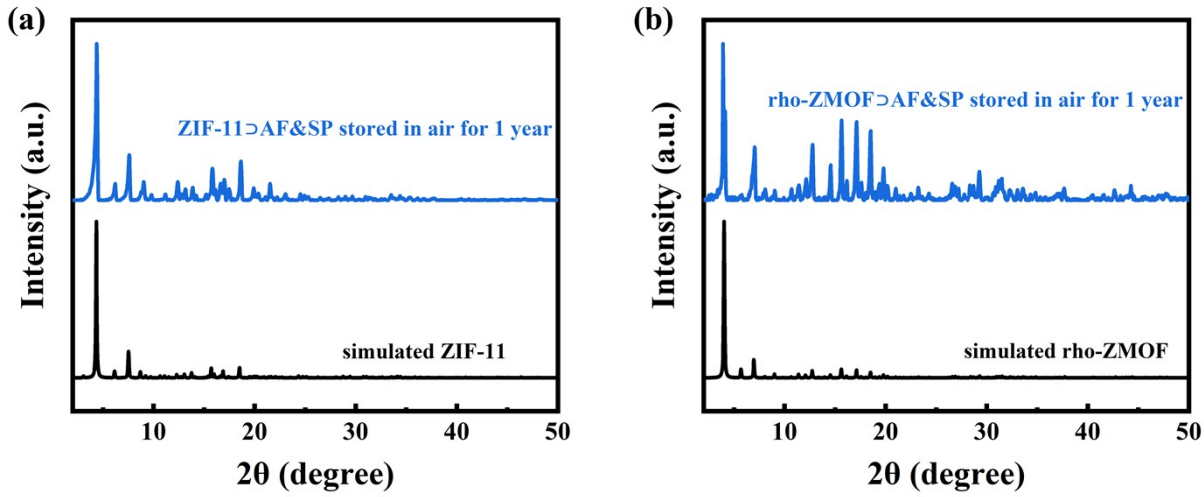

Figure S10. (a) PXRD patterns of simulated ZIF-11 and ZIF-11⊃AF&SP stored in air for 1 year. (b) PXRD patterns of simulated rho-ZMOF and rho-ZMOF⊃AF&SP stored in air for 1 year.

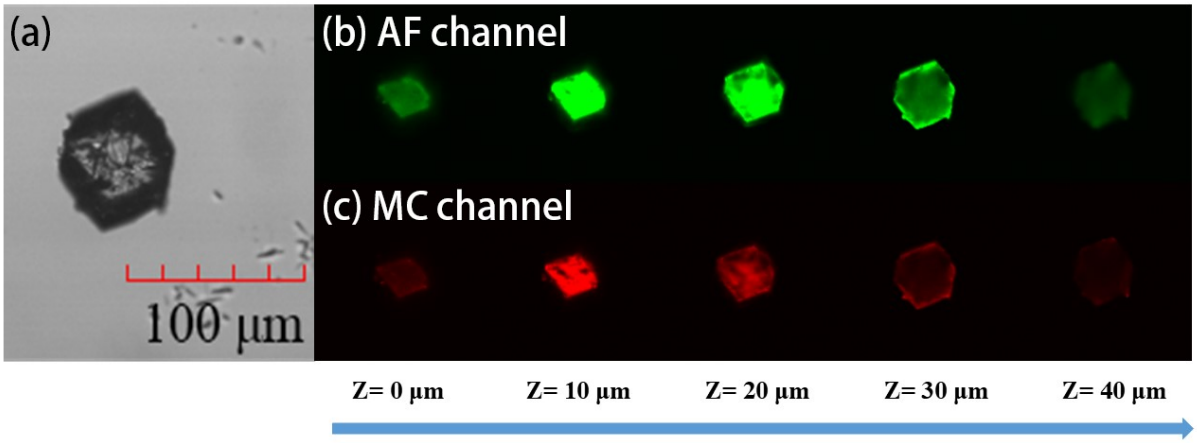

Figure S11. (a) CLSM bright-field images of the rho-ZMOF⊃AF&SP. Scale bar: 100 μm. (b) (c) Fluorescent confocal images of rho-ZMOF⊃AF&SP single crystal at different depths. Excitation wavelength: 488 nm.

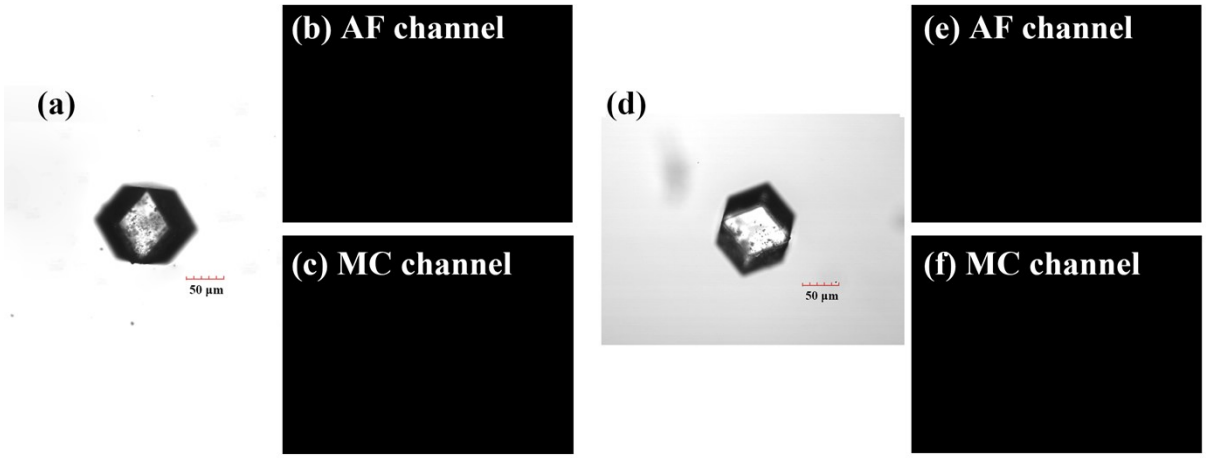

Figure S12. (a) CLSM bright-field images of the ZIF-11. Scale bar: 50 μm. (b) (c) Fluorescent confocal images of ZIF-11. Excitation wavelength: 488 nm. (d) CLSM bright-field images of the rho-ZMOF. Scale bar: 50 μm. (e) (f) Fluorescent confocal images of rho-ZMOF. Excitation wavelength: 488 nm.

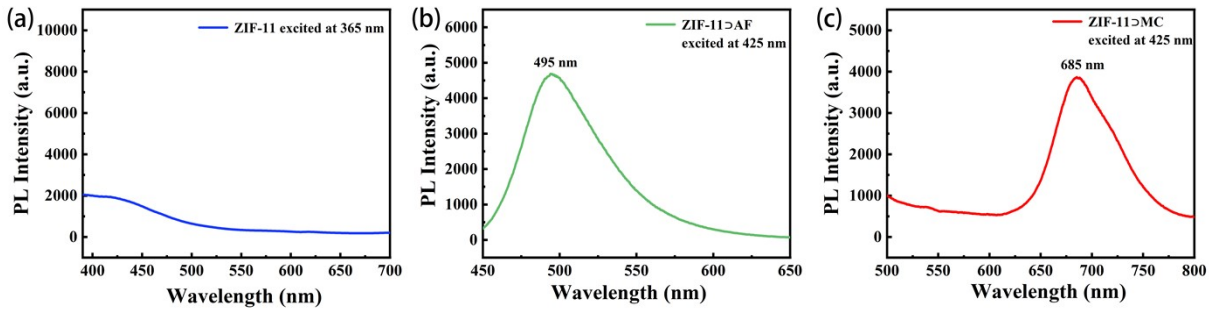

Figure S13. (a) Emission spectra of ZIF-11 excited at 365 nm (b) Emission spectra of ZIF-11⊃AF excited at 425 nm. (c) Emission spectra of ZIF-11⊃MC excited at 425 nm.

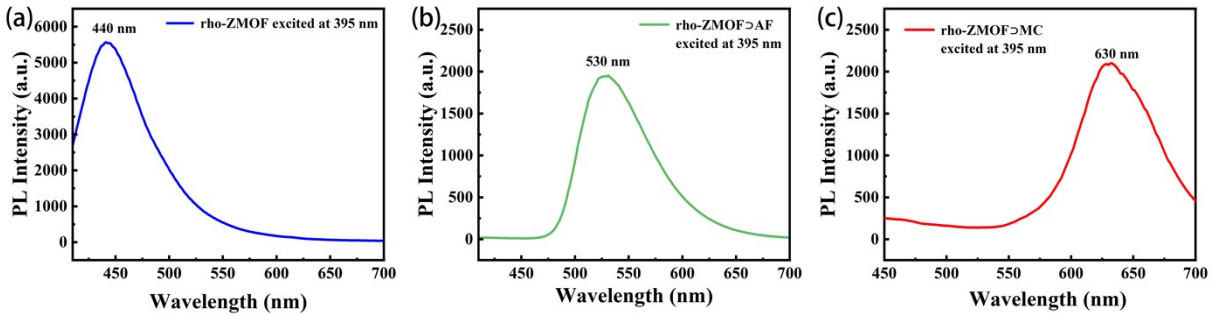

Figure S14. (a) Emission spectra of rho-ZMOF excited at 395 nm. (b) Emission spectra of rho-ZMOF⊃AF excited at 395 nm. (c) Emission spectra of rho-ZMOF⊃MC excited at 395 nm.

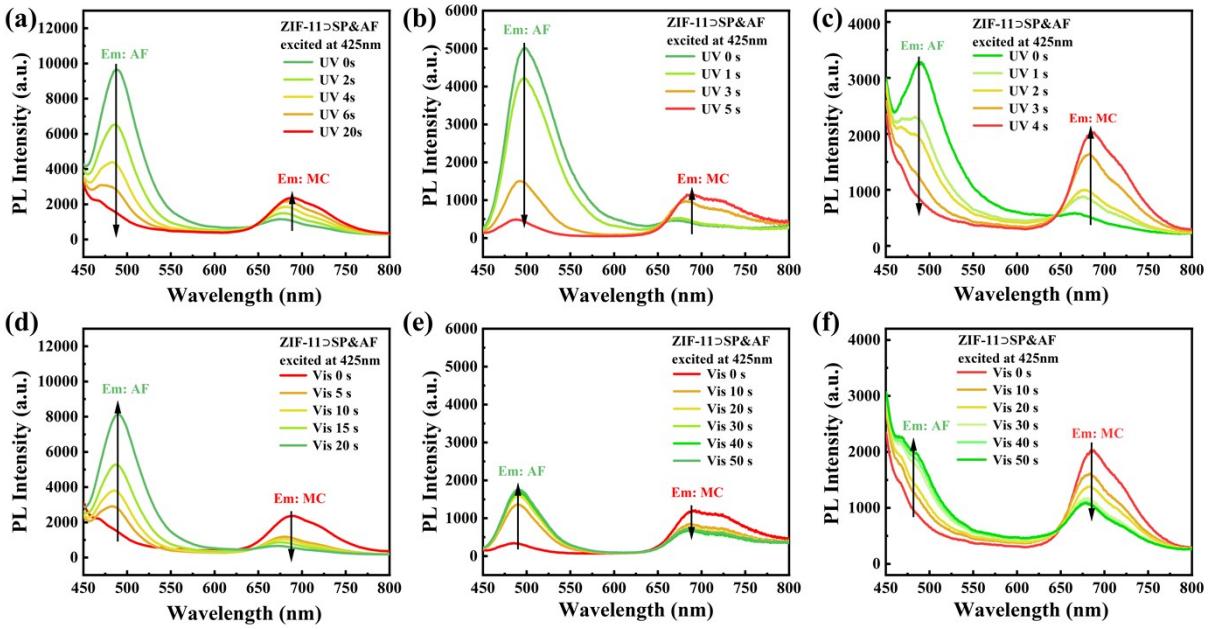

Figure S15. The emission spectra of (a) ZIF-11⊃AF&SP (2.25 wt% AF and 6.61 wt% SP) (b) ZIF-11⊃AF&SP (1.33 wt% AF and 13.44 wt% SP) (c) ZIF-11⊃AF&SP (1.13 wt% AF and 14.76 wt% SP) excited at 425 nm with the addition of UV irradiation times. The emission spectra of (d) ZIF-11⊃AF&SP (2.25 wt% AF and 6.61 wt% SP) (e) ZIF-11⊃AF&SP (1.33 wt% AF and 13.44 wt% SP) (f) ZIF-11⊃AF&SP (1.13 wt% AF and 14.76 wt% SP) excited at 425 nm with the addition of visible light irradiation times.

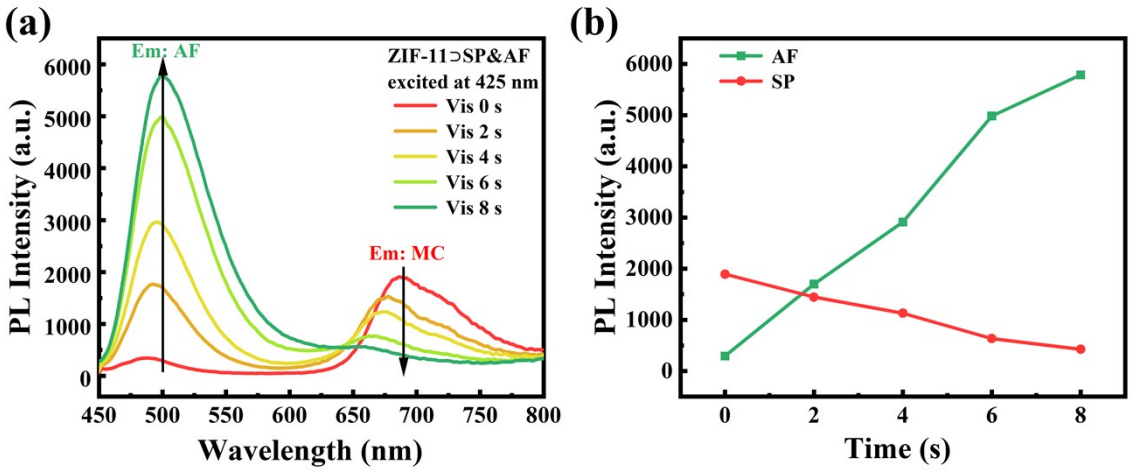

Figure S16. (a) The emission spectra of ZIF-11⊃AF&SP (1.66 wt% AF and 11.30 wt% SP) excited at 425 nm with the addition of visible light irradiation time from 0 to 8 s. (b) Time-dependent fluorescence intensity of AF and SP in ZIF-11⊃AF&SP under visible light irradiation.

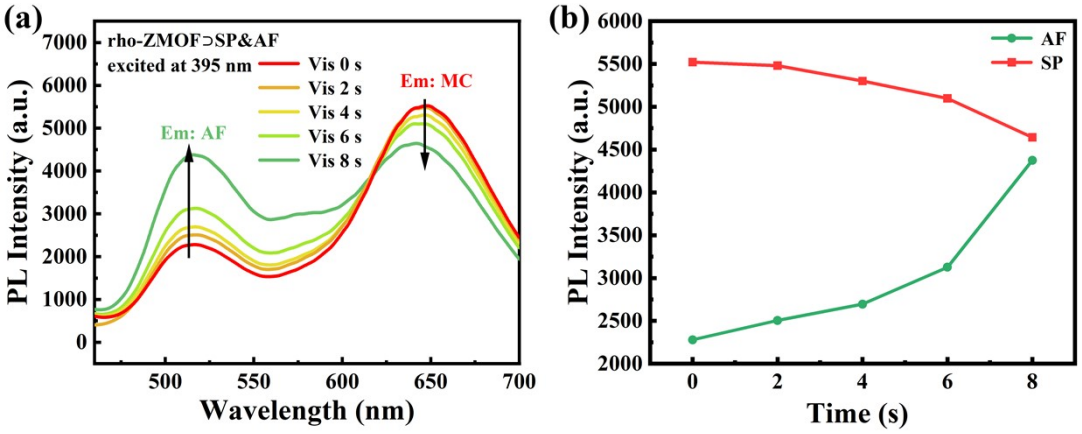

Figure S17. (a) The emission spectra of rho-ZMOF⊃AF&SP excited at 395 nm with the addition of visible light irradiation time from 0 to 8 s. (b) Time-dependent fluorescence intensity of AF and SP in rho-ZMOF⊃AF&SP under visible light irradiation.

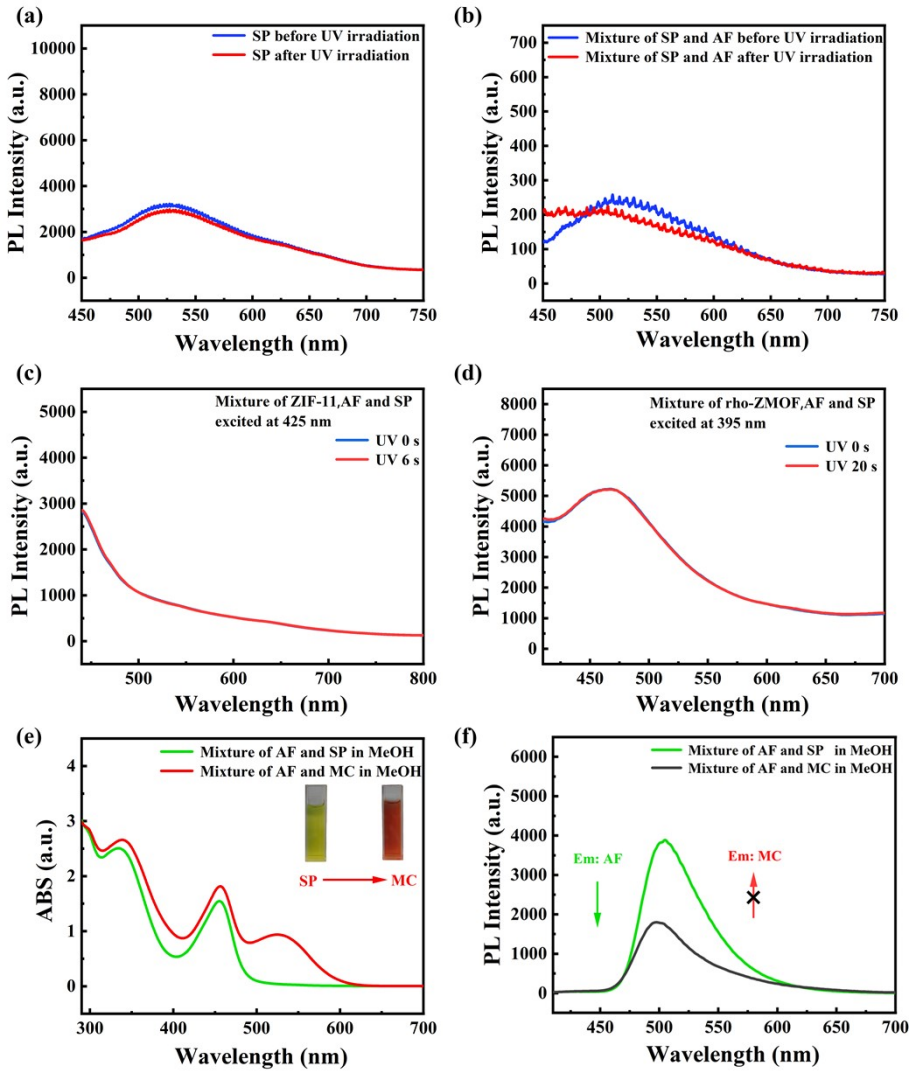

Figure S18. (a) The emission spectra of spiropyran powder before and after UV irradiated for 10 s, excited at 395 nm. The emission spectra of mixture of spiropyran powder and acriflavine powder before and after UV irradiated for 10 s, excited at 395 nm. (c) The emission spectra of mixture of ZIF-11, AF powder and SP powder before and after UV irradiated for 6 s, excited at 425 nm. (d) The emission spectra of mixture of rho-ZMOF, AF powder and SP powder before and after UV irradiated for 20 s, excited at 395 nm. (e) Absorption spectra of a mixture of SP and AF in CH_3CH_2OH solution before and after UV irradiation (SP: 10^{-4} mol L^{-1} AF: 3×10^{-5} mol L^{-1}). (f) Emission spectra of a mixture of SP and AF in CH_3OH solution before and after UV irradiation (SP: 10^{-4} mol L^{-1} AF: 3×10^{-5} mol L^{-1}) excited at 395 nm.

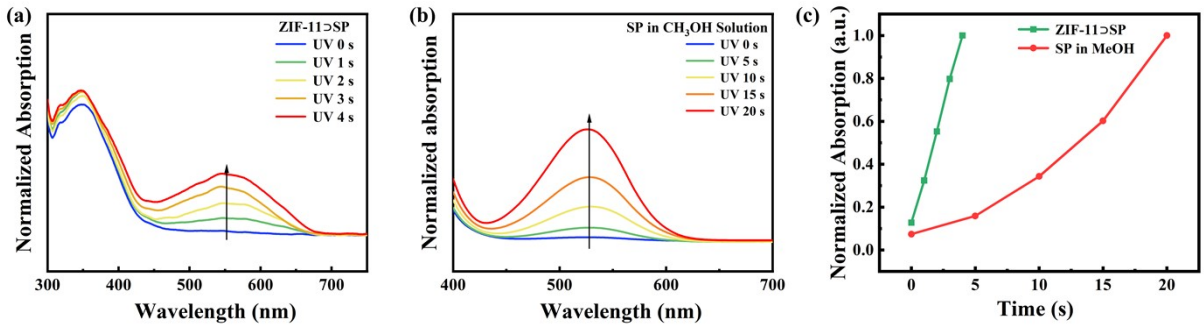

Figure S19. (a) Time-dependent UV-visible diffuse reflectance spectra of ZIF-11⊃SP under UV (365 nm) irradiation. (b) Time-dependent UV-visible absorption spectra of SP in CH_3OH (10^{-4} mol L^{-1}) under UV (365 nm) irradiation. (c) Time-dependent absorption intensity ratio of SP in MeOH and ZIF-11⊃SP under UV (365 nm) irradiation.

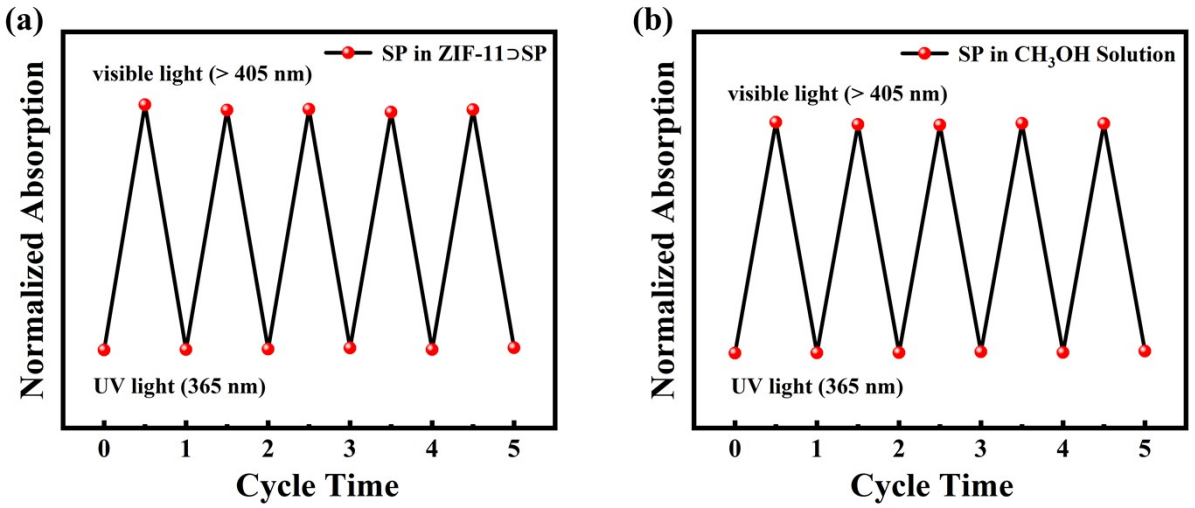

Figure S20. The reversible absorption of (a) ZIF-11⊃SP and (b) SP in CH_3OH (10^{-4} mol L-1) upon alternating UV (365 nm) and visible light (> 405 nm) irradiation.

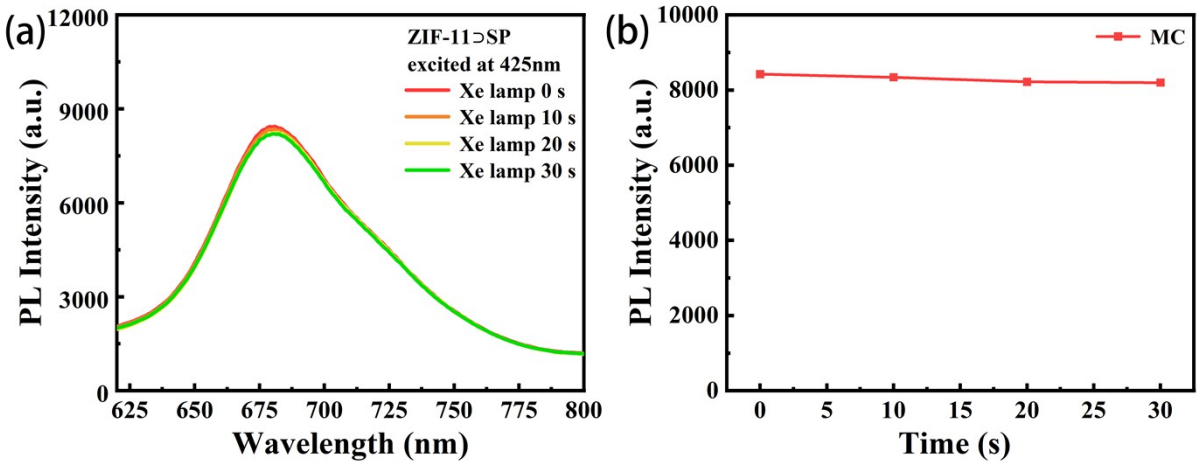

Figure S21. (a) Emission spectra of ZIF-11⊃SP under the irradiation of Xenon lamp excited at 425 nm. (b) Time-dependent fluorescence intensity of SP in ZIF-11⊃SP under the irradiation of Xenon lamp.

.

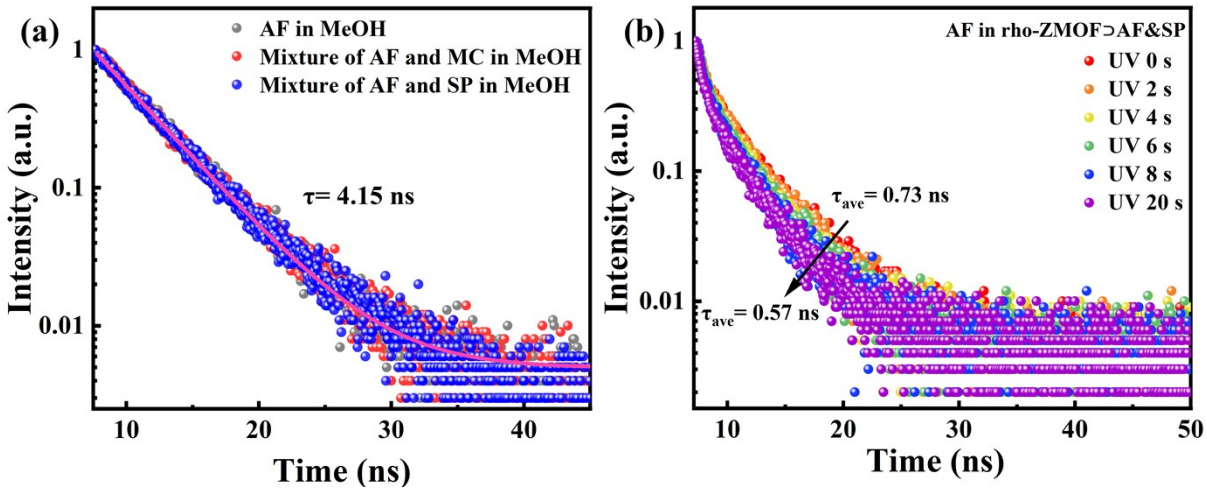

Figure S22. (a) Fluorescence lifetime illustration of AF in CH_3OH (AF: 3×10^{-5} mol L^{-1}) and the Mixture of SP and AF in CH_3OH solution (SP: 10^{-4} mol L^{-1} AF: 3×10^{-5} mol L^{-1}) before and after UV irradiation monitored at 515 nm. (b) Time-dependent fluorescence lifetime variation illustration of AF in rho-ZMOF⊃AF&SP with the addition of UV irradiation times from 0 to 20 s monitored at 520 nm.

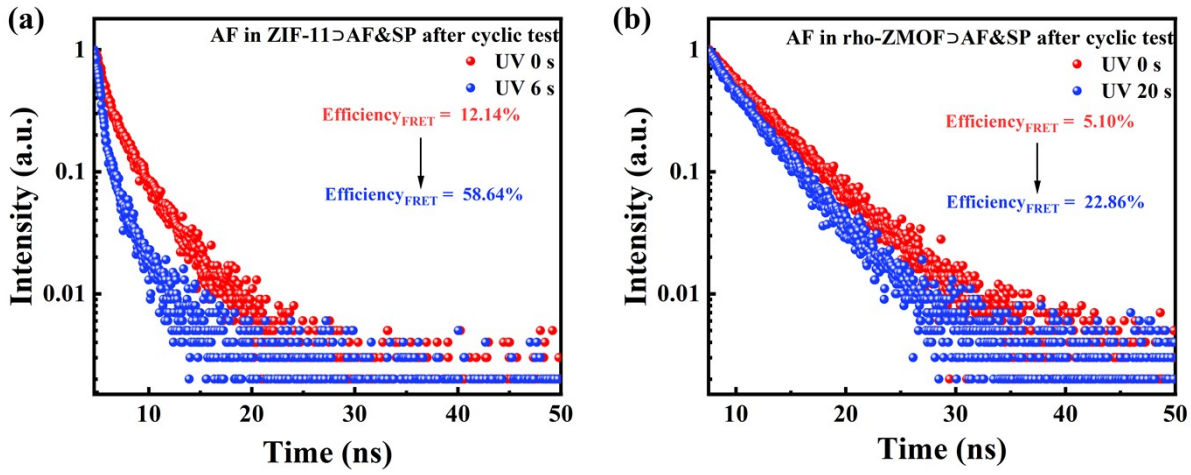

Figure S23. The FRET efficiency variation illustration of (a) ZIF-11⊃AF&SP and (b) rho-ZMOF⊃AF&SP after 5 cyclic tests.

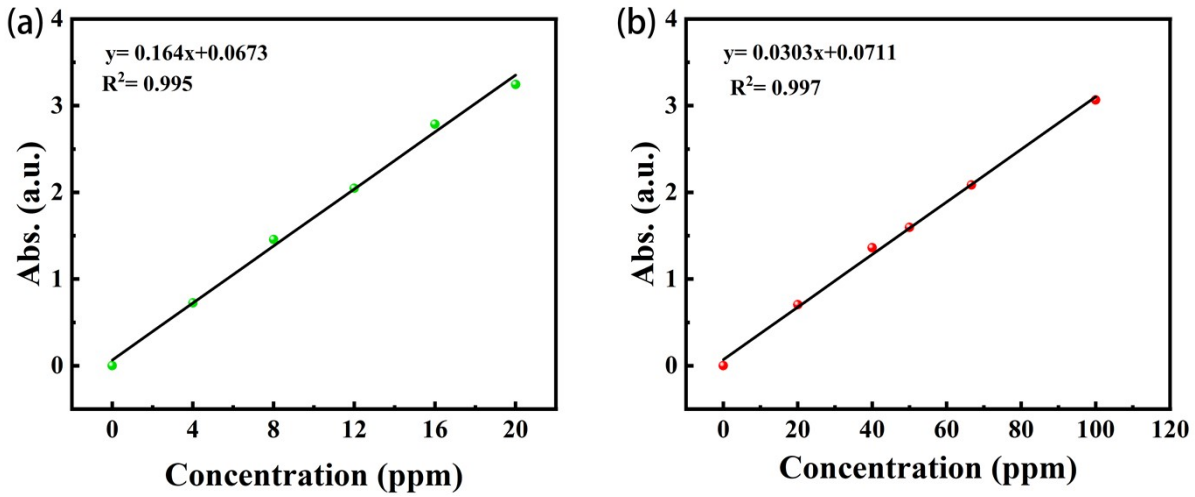

Figure S24. (a) The absorbance-concentration diagram and the fitted curve for the acriflavine solution in CH_3CH_2OH. (b) The absorbance-concentration diagram and the fitted curve for the spiropyran solution in CH_3CH_2OH.

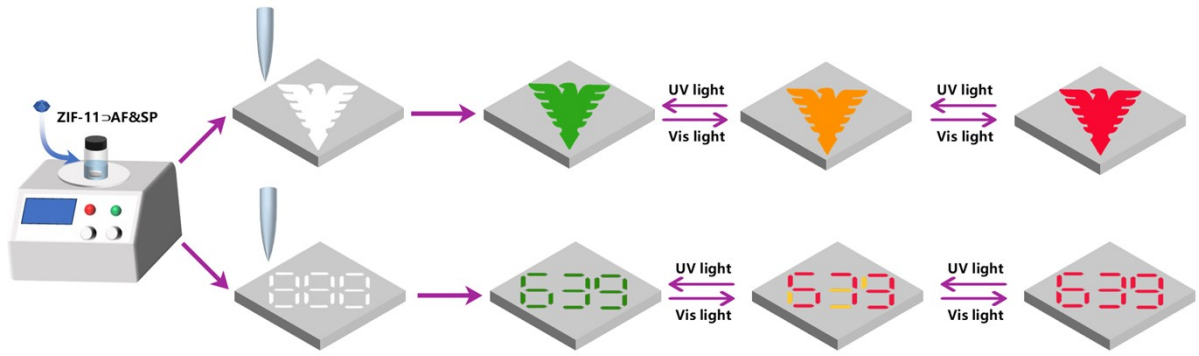

Figure S25. Schematic diagram of the preparation process of ZIF-11⊃ AF&SP-based "Qiushi Eagle" PDMS film and digital time-resolved information encryption process.

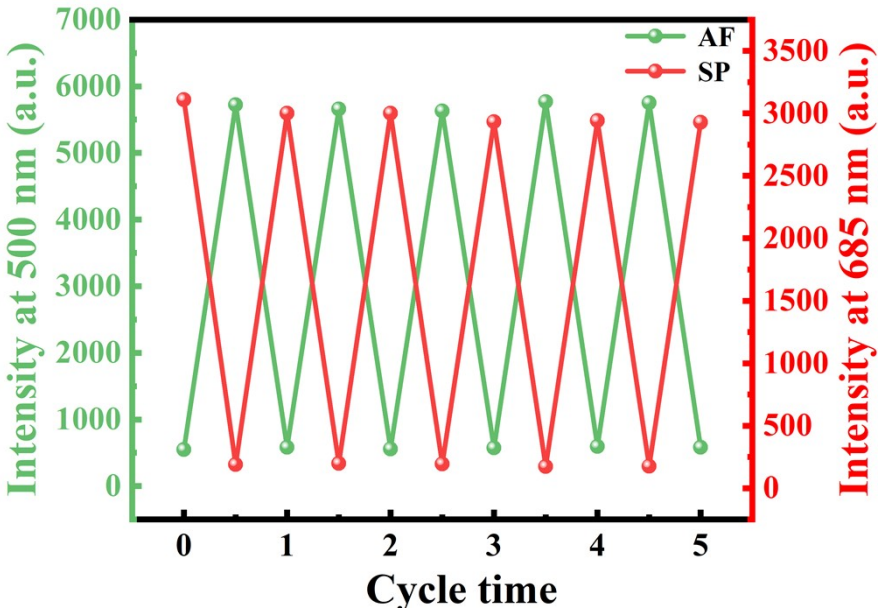

Figure S26. The reversible fluorescence intensity transforms of the PDMS film of ZIF-11⊃AF&SP upon alternating UV (365 nm) and visible light (> 405 nm) irradiation.

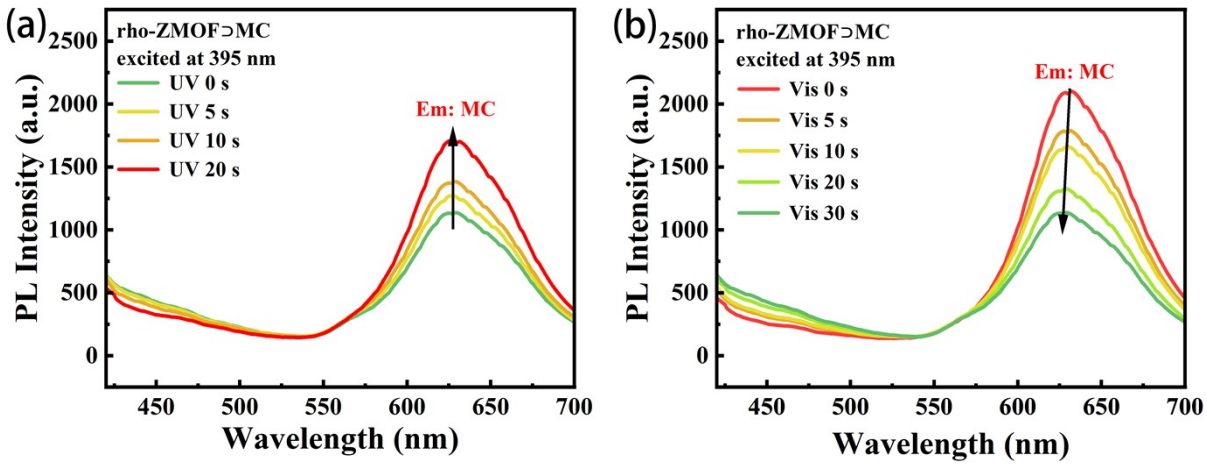

Figure S27. (a) The emission spectra of rho-ZMOF⊃SP excited at 395 nm with the addition of UV irradiation time from 0 to 20 s. (b) The emission spectra of rho-ZMOF⊃SP excited at 395 nm with the addition of visible light irradiation time from 0 to 30 s.

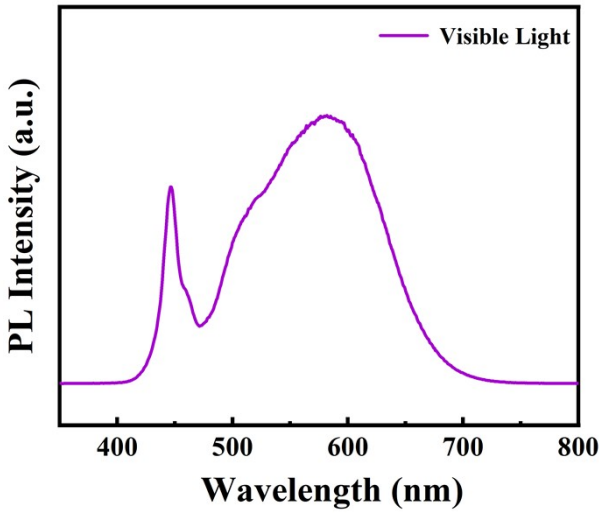

Figure S28. Emission spectra of the visible light (>405 nm) irradiation.